

Effect of residual stress on recrystallization behavior of mechanically alloyed steels

I. Toda-Caraballo¹, J. Chao¹, L.E. Lindgren² and C. Capdevila¹

¹ Materialia Research Group, Department of Physical Metallurgy, Centro Nacional de Investigaciones Metalúrgicas (CENIM-CSIC), Avda. Gregorio del Amo, 8. E-28040 Madrid, Spain

² Division of Computer Aided Design, Luleå University of Technology, S-97187 Luleå, Sweden

Abstract

This paper presents a finite element modeling analysis of deformation on iron-base mechanically alloyed oxide dispersion strengthened alloy by spherical indentations (Brinell test). Results of the model are used to interpret the role of residual shear stresses on the development of recrystallized grain structure and the temperature at which recrystallization occurs.

Keywords: finite element analysis; recrystallization; mechanical alloying; oxide dispersion strengthened alloy; residual stresses.

Mechanical alloying is a process in which mixtures of powders are severely deformed until they form atomic solutions. Inert oxides can also be introduced to form a

1 dispersion of fine particles which strengthen the consolidated product. Significant
2 quantities of iron and nickel-base alloys, with unusual properties, are produced
3 commercially using this process. The total true strain during mechanical alloying can be
4 as large as 9, and there are evidences that this leads to mixing on an atomic scale and to
5 the development of a uniform grain structure which is sub-micrometer in size [1-3].
6 Following mechanical alloying, the particles are consolidated using standard powder
7 metallurgical techniques. The consolidated metal has a very large stored energy,
8 approaching 1 J g^{-1} [4]. This ought to make it easy to induce recrystallization, but in
9 practice the alloys fail to recrystallize except at very high temperatures close to melting
10 [2]. On the other hand, the recrystallization temperature can be reduced dramatically by
11 slightly deforming the consolidated product prior to heat treatment [5]. It is in this
12 context that the effect of deformation on PM 2000 by spherical indentations (Brinell
13 test) on the development of recrystallized grain structure is studied here.

14 The Fe-base oxide dispersion strengthened PM 2000 ($\text{Fe-20Cr-6Al-0.5Ti-0.5Y}_2\text{O}_3$),
15 supplied by PLANSEE GmbH, is created by mechanical alloying. The powders with a
16 grain size of about 70 nm were therefore consolidated by hot isostatic pressing and
17 subsequently by hot rolling of vacuum – sealed cans at about 1000 °C to form a 7 mm
18 wall-thickness tube. During this stage dynamic recovery and recrystallization occur to
19 produce a mixture of elongated deformed grains and relatively equiaxed recrystallized
20 grains with a sub-micrometric grain size in the transverse direction and a strong $\langle 110 \rangle$ -
21 fibre texture [6-7]. Prismatic samples of 60 mm in length and $20 \times 7 \text{ mm}^2$ section have
22 been machined from the tube in as-received condition to perform spherical indentations
23 at the inner wall. A 10 mm in diameter spherical indenter has been used. Loads ranging
24 from 4.9 to 49 kN have been applied. Hereafter, the Brinell tested material is referred as
25 deformed material.

1 A systematic study of the early stages of recrystallization as a function of annealing
 2 temperature and deformation was carried out. Table 1 lists the temperature at which
 3 recrystallization starts (T_R) after isochronal (3 hours) heat treatments at different
 4 annealing temperatures. It could be concluded that the higher the deformation induced,
 5 the lower the temperature at which recrystallization is detected. The recrystallization
 6 temperature in absence of deformation was determined at 1330 °C. The first observable
 7 result is seen in the case of 4.9 kN at 1320°C. The higher deformation produced in the
 8 test of 49 kN induces recrystallization at temperature as low as 1150°C.

21 Table 1. T_R values vs. Brinell load after three hours isochronal heat treatments

Brinell test loads (kN)	T_R (°C)
49.0	1150
29.4	1210
19.6	1250
4.9	1320
0	1330

41 Optical microscopy analysis on non- recrystallized samples reveled that a very
 42 elongated and coarse-grained microstructure, characteristic of a secondary
 43 recrystallization process in ferritic ODS alloys [8-11], is developed. Regarding
 44 deformed samples, it was observed that the lower the deformation, the bigger the grain
 45 size and fewer the number of recrystallized grains that appear in the microstructure. In
 46 the area affected by deformation, the recrystallized grain is equiaxed in the early stages,
 47 but following growth in the parallel direction to the surface produces elongated grains
 48 which finally coarsen in the normal direction to the surface. Figure 1 illustrates the

1 effect of increasing deformations on subsequent recrystallization of PM 2000. It is
2 evident the effect of the deformation magnitude on the recrystallization, since the bigger
3 the indentation load, the more extended the volume of recrystallized material and finer
4 the recrystallized grain size.
5
6
7

8
9 These results are consistent with the ones reported by Nutting [8] and Capdevila et al
10 [1]. Nutting studied the recrystallization process in a 60% cold worked sheet which was
11 slightly deformed by bending, and claimed that recrystallization was triggered in places
12 subjected to residual compressive stresses [8]. Capdevila reported a two fold effect on
13 the recrystallization behavior of specimens subjected to different bending angles: As
14 cold deformation increases it was noted a decrease in the recrystallization temperature
15 and an increase in the density of recrystallization nuclei disregarding of the stress
16 direction [1].
17
18
19
20
21
22
23
24
25
26
27

28 Recrystallization requires volumetric free energy terms of stored energy of dislocations
29 to drive the migration of the boundaries around the growing grains. When the material
30 is under stress there are additional terms and it is these which we will concentrate on
31 here. It was noted that both the velocity and the direction of migration of high angle
32 boundaries varied, depending on their misorientation [12]. It is possible to interpret
33 these results in terms of applied stress acted to drive the movement of structural
34 dislocations in the boundary [13]. It was also noted that the migration mechanism of
35 grain boundary motion is different in a stressed material than the mechanism of
36 curvature driven grain boundary motion (or texture induced) in a non-stressed material
37 [13-15]. During indentation the material flow occurs in the extrusion direction, so it is
38 assumed that no texture change takes place. These facts and the grains morphology due
39 to extrusion process suggest the special importance to the shear stress component of the
40 beginning of recrystallization.
41
42
43
44
45
46
47
48
49
50
51
52
53
54
55
56
57
58
59
60
61
62
63
64
65

1 In order to discern the effect of the residual stress on the recrystallization a Finite
2 Element Modeling (FEM) is performed by the multipurpose finite element program
3 MSC.Marc provided by Luleå University of Technology. The results were analyzed
4 comparing the aspect of the recrystallized zones with those of the iso-strain and σ_{xy} iso-
5 stress contours. Although Von Mises stress is related to dislocation glide, the glide
6 related to parallel to grain boundaries are more important. Von Mises stress is isotropic
7 and will miss the influence of the larger amount of grain boundaries parallel with the x-
8 axis. As it was described above, the material flow is not isotropic, but occurring in
9 extrusion direction. For this reason the stress analysis described below is focused on the
10 σ_{xy} shear stress component distribution instead of Von Mises stress distribution, which
11 its isotropic character will miss the anisotropy of the grain boundary movement.

12 The simulations were performed considering a spherical steel ball of 5mm in radius as
13 indenter with isotropic linear elastic behavior. The contact between spherical indenter
14 and sample was modeled as Coulomb friction with a friction coefficient of 0.1. The
15 loads considered in calculations were ranging from 4.9 to 49 kN. Simulations were
16 performed on a 7 mm in thickness and 30 mm in length sample considering a mesh with
17 cylindrical symmetry (axial symmetry around the centre of the indenter in the vertical
18 direction). The sample was modelled as an elastoplastic material with isotropic Von
19 Mises yield criterion and with isotropic work hardening in which the Young's modulus
20 was 210 GPa and the Poisson's ratio was 0.3. The flow stress curve defined by the
21 expression

$$\sigma = 1000 + 865.7\bar{\epsilon}_p^{0.505} \quad (1)$$

22 was obtained by fitting to experimental data. In this expression σ is the true flow stress
23 (in MPa) and $\bar{\epsilon}_p$ is the true plastic strain. The model accounts for large deformations

1 and strains using an updated Lagrangian formulation and a finite strain model derived
2 from the incremental theory of plasticity.
3

4 Of particular interest is the state of deformation at the temperature when
5 recrystallization is triggered for a given load. At this state the residual stress at the
6 unloaded state are allowed to move and relax. For this reason, the residual stress
7 evolution (function of the initial unloaded state and temperature) during recrystallization
8 heat treatment, has been analyzed using the finite element method and the constitutive
9 equation proposed by Johnson – Cook [16]. In this sense, the evolution with
10 temperature of equation (1) could be expressed as follows:
11
12
13
14
15
16
17
18
19
20
21
22
23

$$\sigma = (A + B\bar{\epsilon}_p^n) \left(1 + C \ln \frac{\dot{\bar{\epsilon}}_p}{\dot{\bar{\epsilon}}_0} \right) \left(1 - \left(\frac{T - T_r}{T_m - T_r} \right)^m \right) \quad (2)$$

24
25
26
27
28
29
30
31 The parameters A , B , and n are those defining the stress-strain curve at (1), C is the
32 strain-rate coefficient considered as 1.5×10^{-2} [17], $\dot{\bar{\epsilon}}_0$ is the initial plastic strain rate with
33 a reference value of 10^{-4} s^{-1} and $\dot{\bar{\epsilon}}_p$ is the plastic strain rate. The effect of the
34 temperature is defined through T (current temperature), T_r (room temperature, i.e. 25
35 °C), T_m (melting temperature, i.e. 1487 °C) and the thermal softening constant (m)
36 considered as 0.6 [18]. Moreover, it was checked the negligible effect of Young's
37 modulus temperature dependence on calculations.
38
39
40
41
42
43
44
45
46
47
48

49 Figure 2 shows a comparison between a shear residual stress (σ_{xy}) map and the early
50 stages of recrystallization in a deformed and subsequently heat treated at 1150 °C / 3h
51 sample. It is clearly observed in this figure that the recrystallized zones (Fig. 2(b))
52 match with those where σ_{xy} presents the highest values. This illustrates the role of shear
53 stresses on recrystallization of Fe-base mechanically alloyed steels. However, it is clear
54
55
56
57
58
59
60
61
62
63
64
65

1 from Fig. 1 that the nucleated grain tends to grow towards the area affected by
2 indentation but not the surrounding unaffected area. Thus, residual shear stress trigger
3 the nucleation of recrystallization and the recrystallized grains grow in the higher
4 deformed material, which is consistent with the total strain energy map showed in Fig.
5 2(c).
6
7
8
9

10 Figure 3 shows the evolution of the ratio between σ_{xy} and τ_0 (shear yield strength), i.e. δ
11 = σ_{xy} / τ_0 , with temperature. The shear stress values considered corresponds to the zone
12 where start of recrystallization has been detected. Therefore, once δ reaches the value of
13 one, the residual shear stress would be high enough to drive the dislocation movement,
14 and hence to induce the movement of grain boundaries, which burst the recrystallization
15 process. This is consistent with the idea described by Hutchinson and Wynne [18]
16 where it is described that boundary movement is accompanied by shearing of the
17 volume through which a boundary moves. While any high angle boundary may be
18 formally described by a dislocation arrangement, it is not so evident which dislocations
19 are actually involved, and how to resolve the stress that drives them. In this case, it may
20 be easier to think of structural units and coordinated jumps of atoms across the
21 boundary providing the mechanism for migration. Which ever view point is adopted, it
22 is important to remember that energy has to be supplied to provide that which is being
23 dissipated during the boundary migration. This can only come from work done by the
24 component of force acting parallel to the boundary and so shearing must always
25 accompany migration when this is stress-driven, whatever the misorientation of the
26 boundary. Since each element of grain boundary is an invariant plane, the only possible
27 work is by translation parallel to the boundary or, in other words, by shearing the
28 volume as the boundary passes through it. In this case, the significant stress component
29 will be a shear stress parallel to the boundary. The maximum possible driving force in
30
31
32
33
34
35
36
37
38
39
40
41
42
43
44
45
46
47
48
49
50
51
52
53
54
55
56
57
58
59
60
61
62
63
64
65

1 this case is then equal to the work done per unit volume $\gamma\sigma_{xz}$ where γ is the shear strain
2 accomplished, which depend on the misorientation and structure of the boundary.
3

4 Figure 4 shows a correlation between the corresponding temperatures at which δ
5 becomes one, and the recrystallization temperatures listed in Table 1. The good
6 agreement between both values allows us to conclude that shear stresses could be a
7 parameter controlling the nucleation of recrystallisation in mechanically alloyed steels.
8
9

10 In summary, the presence of residual shear stresses at the moment of recrystallization
11 boosts the grain boundary movement and hence reduces the recrystallization
12 temperature. The quantification of the parameter that governs the recrystallization in
13 PM2000 ODS steel has been fixed when the ratio δ reaches the value of one.
14
15
16
17
18
19
20
21
22
23
24
25
26

27 **Acknowledgements**

28 I. Toda Caraballo acknowledges the Spanish Ministerio de Ciencia e Innovación for
29 financial support in the form of PhD research grant (FPI). The authors acknowledge
30 financial support for this investigation from the Spanish Ministerio de Educación y
31 Ciencia through the Plan Nacional 2006 ENE2006-15170-C02-01/ALT.
32
33
34
35
36
37
38
39
40
41
42

43 **References**

- 44
45
46 [1] C. C. Montes and H.K.D.H. Bhadeshia, Adv. Eng. Mater. 5 (2003) 232.
47
48 [2] C. Capdevila and H.K.D.H. Bhadeshia, Adv. Eng. Mater. 3 (2001) 647.
49
50
51 [3] C. Capdevila, U. Miller, H. Jelenak and H.K.D.H. Bhadeshia, Mater. Sci. Eng. A
52 316 (2001) 161.
53
54
55
56 [4] T. S. Chou and H. Bhadeshia, Mater. Sci. Eng. A 189 (1994) 229.
57
58 [5] H. Regle and A. Alamo, J. Phys. IV 3 (1993) 727-731.
59
60
61
62
63
64
65

- 1
2
3
4
5
6
7
8
9
10
11
12
13
14
15
16
17
18
19
20
21
22
23
24
25
26
27
28
29
30
31
32
33
34
35
36
37
38
39
40
41
42
43
44
45
46
47
48
49
50
51
52
53
54
55
56
57
58
59
60
61
62
63
64
65
- [6] C. Capdevila, Y. L. Chen, N. C. K. Lassen, A. R. Jones and H.K.D.H. Bhadeshia, Mater. Sci. Technol. 17 (2001) 693.
 - [7] C. Capdevila, Y. L. Chen, A. R. Jones and H.K.D.H. Bhadeshia, ISIJ Int. 43 (2003) 777.
 - [8] J. Nutting, S. Ubhi, T.A. Hughes. Proc. Int. Conf. on Oxide Dispersion Strengthened Superalloys by Mechanical Alloying, J.S. Benjamin (Ed), IncoMAP, 1981 33-41.
 - [9] C. Capdevila, Metall. Mater. Trans. A 36A (2005) 1547.
 - [10] C. Capdevila, J. P. Ferrer, F. G. Caballero and C. Garcia de Andres, Metall. Mater. Trans. A 37A (2006) 2059.
 - [11] J. L. Gonzalez-Carrasco, J. Chao, C. Capdevila, J. A. Jimenez, V. Amigo and M. D. Salvador, Mater. Sci. Eng. A 471 (2007) 120.
 - [12] C.H. Li, E.H. Edwards, J. Washburn and E.R. Parker, Acta Metall. 1 (1953) 223.
 - [13] M. Winning, G. Gottstein and L.S. Shvindlermann, Acta Mater. 49 (2001) 211.
 - [14] M. Winning, Acta Mater. 51 (2003) 6465.
 - [15] M. Winning, G. Gottstein and L.S. Shvindlerman, Acta Mater. 50 (2002) 353.
 - [16] G.R. Johnson, W.H. Cook, Proc. 7th Int. Symp. on Ballistic. Publ. The Hague, The Netherlands. 1983 541-547
 - [17] H. Chang and I. Baker, Metall. Mater. Trans. A 38A (2007) 2815.
 - [18] B. Hutchinson and B. Wynne, Mater. Sci. Forum 550 (2007) 149.

Figure Captions

1
2
3
4
5 Figure 1: Recrystallized microstructure of deformed area after annealing at 1350 °C for
6
7 3 h: (a) 4.9 kN and (b) 49 kN. Transverse section to extrusion direction.
8
9

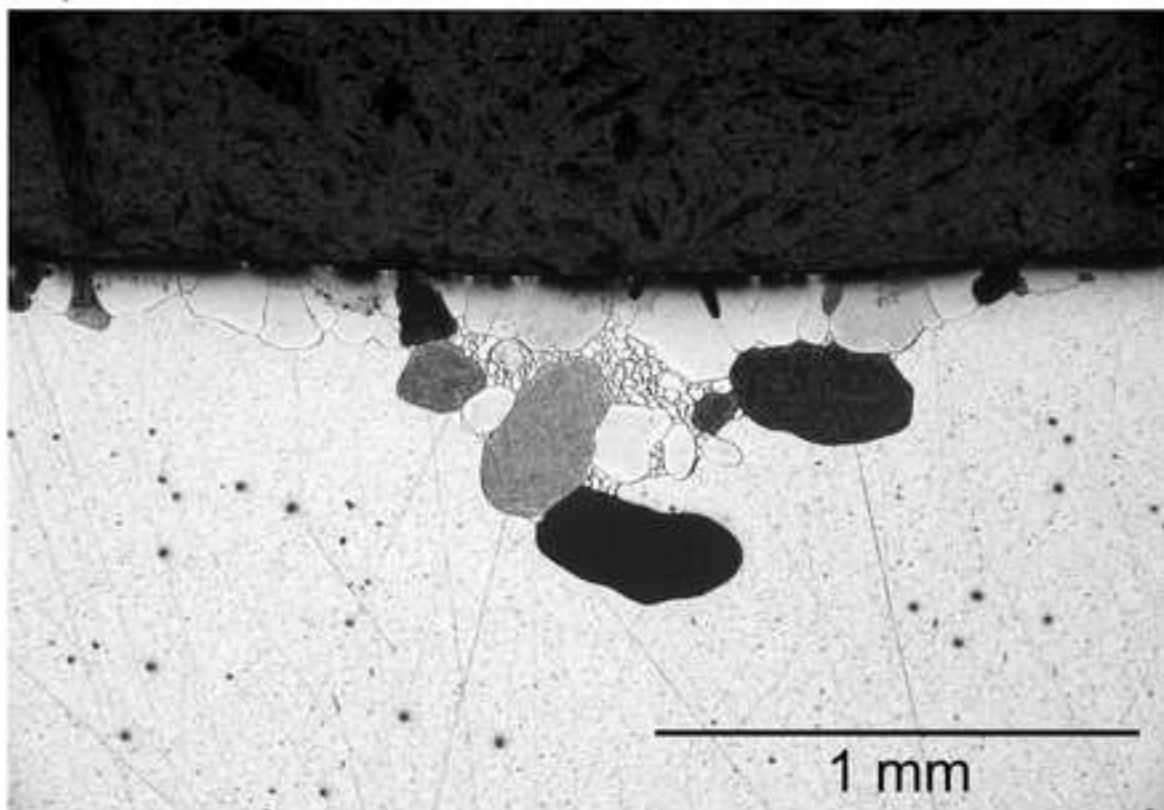
10
11
12 Figure 2: (a) σ_{xy} map at 1150 °C after deformation for 49 kN load, (b) recrystallization
13
14 microstructure after 49 kN load and subsequent annealing at 1150 °C for 3 h, and (c)
15
16 strain energy density map for 49 kN indentation load.
17
18
19
20

21
22 Figure 3: Evolution of δ with temperature
23
24
25

26
27 Figure 4: Correlation between experimental T_R and temperatures at which $\delta = 1$ (T_δ).
28
29
30
31
32
33
34
35
36
37
38
39
40
41
42
43
44
45
46
47
48
49
50
51
52
53
54
55
56
57
58
59
60
61
62
63
64
65

Figure 1
[Click here to download high resolution image](#)

a)



b)

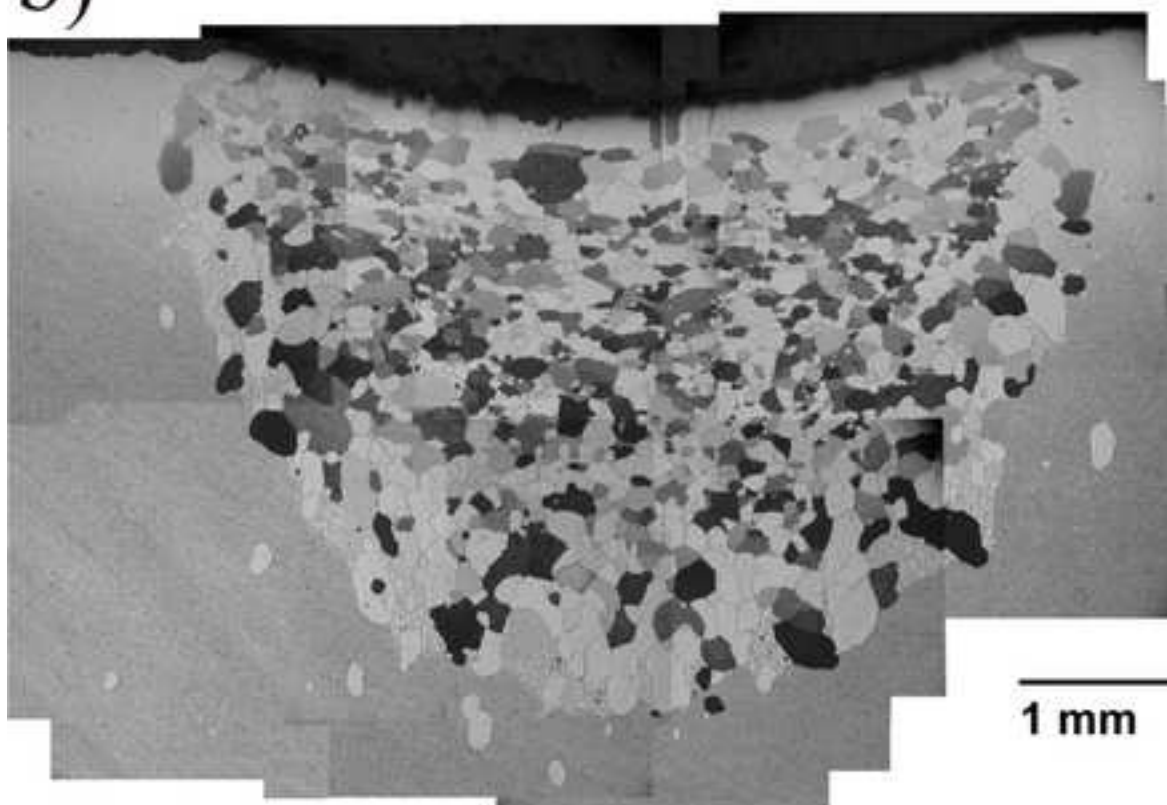


Figure 3
[Click here to download high resolution image](#)

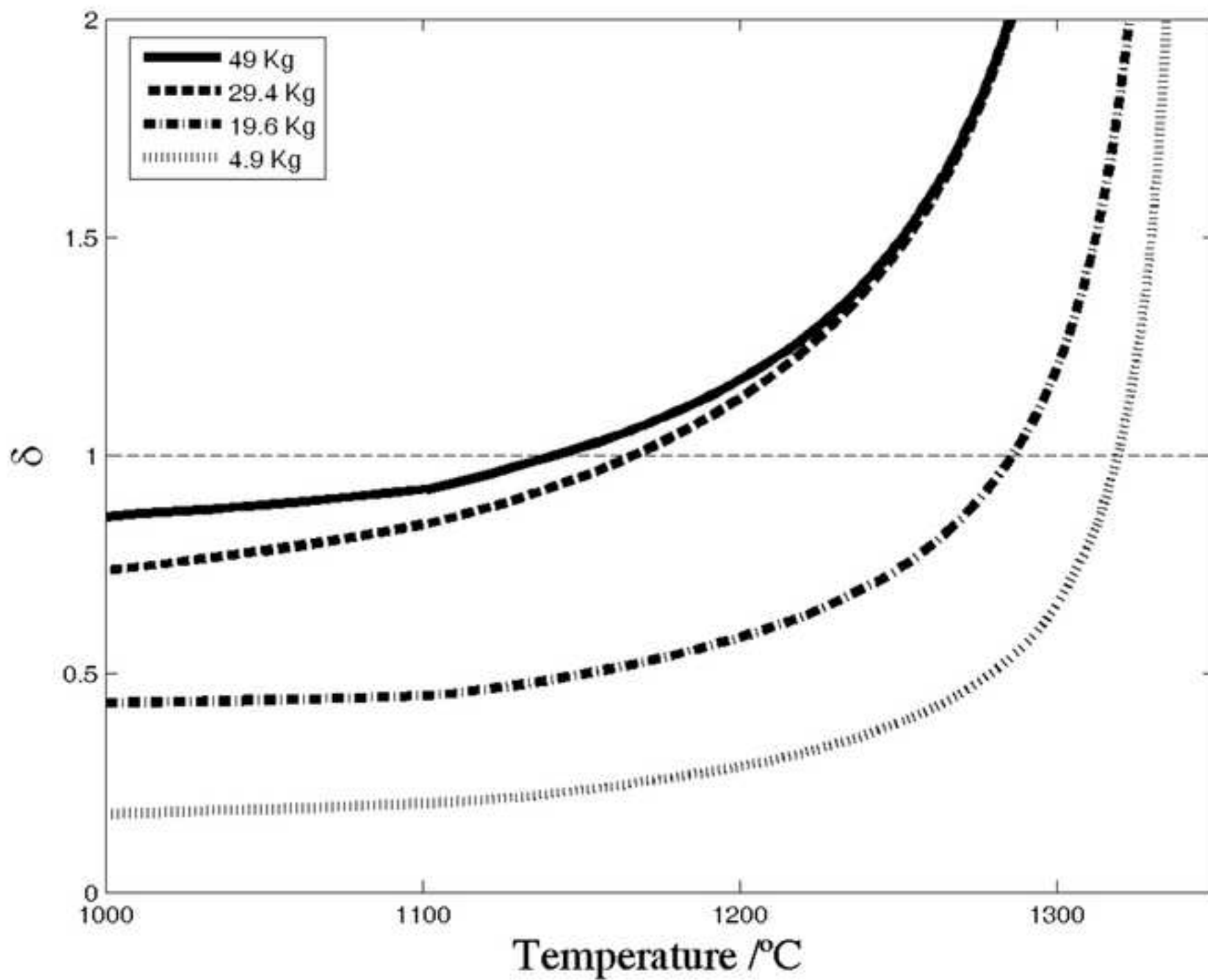


Figure 4
[Click here to download high resolution image](#)

